Title	A laser-micromachined polymeric membraneless fuel cell
Author(s)	Li, Aidan; Chan, Siew Hwa; Nguyen, Nam-Trung
Citation	Li, A., Chan, S. H., & Nguyen, N. T. (2007). A laser-micromachined polymeric membraneless fuel cell. Journal of Micromechanics and Microengineering, 17(6), 1107.
Date	2007
URL	http://hdl.handle.net/10220/7820
Rights	© 2007 IOP Publishing Ltd. This is the author created version of a work that has been peer reviewed and accepted for publication by Journal of Micromechanics and Microengineering, IOP Publishing Ltd. It incorporates referee's comments but changes resulting from the publishing process, such as copyediting, structural formatting, may not be reflected in this document. The published version is available at: DOI: [http://dx.doi.org.ezlibproxy1.ntu.edu.sg/10.1088/0960-1317/17/6/002].

Laser-micromachined polymeric membraneless fuel cell

Aidan Li, Siew Hwa Chan, Nam-Trung Nguyen§

Fuel Cell Strategic Research Programme, School of Mechanical and Aerospace Engineering, Nanyang Technological University, 50 Nanyang Avenue, Singapore 639798

Abstract. This paper presents a laser-micromachined polymeric membraneless fuel cell. The membraneless fuel cell, constructed with three polymethyl methacrylate (PMMA) layers, takes advantage of two laminar flows in a single micro channel to keep the fuel and oxidant streams separated yet in diffusional contact. Laser micromachining was employed to make the flow channel and electrode substrate based on PMMA. The anode and cathode electrodes were fabricated by wet-spraying catalyst inks onto the gold-coated PMMA substrate. The packed fuel cell has been electrochemically characterized by an electrochemical analyzer. The membraneless fuel cell works stably with Reynolds numbers ranging from 7.65 to 30.6. At room temperature, the laminar-flow-based micro membraneless fuel cell can reach a maximum power densities of 0.58 mW/cm^2 with 0.5 M HCOOH in 0.1 M H_2SO_4 solution as fuel and O_2 saturated 0.1 M H_2SO_4 solution as oxidant. When 0.01 M H_2O_2 in 0.1 M H_2SO_4 solution is used as oxidant, a maximum power density of 1.98 mW/cm^2 is obtained. The paper reports for the first time the use of hydrogen peroxide in sulfuric acid as the oxidant. The new oxidant composition allows a simple recycling process and a better fuel utilization.

§ To whom correspondence should be addressed (mntnguyen@ntu.edu.sg)

1. Introduction

The widespread use of portable electronic devices stimulates the rapid development of miniature power sources. Among them, micro fuel cells become more and more attractive due to their advantages of high energy-conversion efficiency, and capability of producing electricity as long as fuel and oxidant are supplied to the electrodes [1]. Miniaturization technology and fuel storage are the two critical issues for the successful development of micro fuel cells. Silicon-based microtechnologies previously used for the fabrication of microelectromechanical systems (MEMS) and advanced integrated circuits (IC) have been widely employed to make micro fuel cells [2, 3, 4, 5]. However, compared to MEMS and IC, the relative large size of fuel cells make the cost per device very high. Mass fabrication of micro fuel cells based on polymeric materials is a more economic solution. In the past, we have successfully developed fully polymeric microfluidic components such as microvalves [6] and micropumps [7]. Together with a fully polymeric micro fuel cell [8], we have proved that complex polymeric micro fuel cells can be built at low costs.

Although hydrogen is one of the best fuels for polymer electrolyte membrane fuel cells (PEMFCs), especially for macroscale systems, the dimension, weight and safety concerns of the high-pressure hydrogen tank prevent their successful miniaturization. Ideal fuels for micro fuel cells should be in liquid form at ambient temperature. Methanol and formic acid are the two typical examples of liquid fuels.

Extensive studies have been reported on the development of micro direct methanol fuel cells (μDMFC) and formic acid fuel cells (μFAFC) due to the convenient storage of the liquid fuels [4, 5]. Most of the previous studies were based on the conventional Nafion membrane as the electrolyte to separate the fuel and oxidant and to conduct protons between the anode and the cathode. Performance deterioration and fuel crossover, especially when running methanol, are the intrinsic problems associated with the Nafion membrane [9]. Although some works have focused on developing methanol-tolerant cathode materials or/and innovative membrane materials less permeable to methanol, their intrinsic activity is currently too low to make a significant difference to the overall cell performance [10]. Recently, some novel designs, such as bio-fuel cell and laminar-flow-based membraneless fuel cell, have been proposed to avoid the membrane-associated problems by removing the conventional PEM. Employing the selective catalysts, generally enzymes, to restrict the reaction of oxidant and reductant to the appropriate electrode, bio-fuel cells can operate with both oxidant and fuel present in a mixture [11, 12]. Bio-fuel cells have received increasing interests because they use biological enzymes instead of precious metals as catalysts. This fact may allow bio-fuel cells to be implanted in living organisms. The drawback of bio-fuel cells is the relatively low output power due to the low electrocatalytic activity of the enzyme electrodes, which is in the range from several μW/cm^2 to several hundred μW/cm^2 [11, 12].

The concept of the membraneless micro fuel cell based on laminar flow was first demonstrated by Ferrigno et al. [13] using vanadium redox couples as fuel and oxidant.

Because pressure-driven flow in microchannels is generally laminar, has low Reynolds numbers and reasonability high Peclet number [14], two streams containing oxidant and fuel can be separated because the dominant convective transport. Thus, ions can diffuse through the liquid-liquid interface similar to the case of a membrane interface. Currently, two designs exist for laminar flow based membraneless microchannel fuel cells. The first design is a Y-shaped microchannel with oxidant and fuel flowing side by side [15, 16, 17]. With this design, the fabrication of the electrode on the side wall is challenging. The second design lets the fuel and oxidant on the top and bottom of the micro channels [18, 19]. With this design, electrodes can be fabricated using conventional coating techniques on a substrate surface. In most cases, polydimethylsiloxane (PDMS) or silicon were used as the substrate for these membraneless micro fuel cell. Microtechnologies such as soft lithography [15] or standard photolithography [18] were employed for microchannel fabrication. The fabrication requires specialized clean-room facilities. Furthermore, the small dimension of the microchannels makes the integration of electrodes is challenging. Choban et al. [15] fabricated the electrodes using electron-beam evaporation of platinum. Cohen et al [18] used electrodeposition of platinum black to form the electrodes. In general, both designs requires complicated fabrication processes for the microchannels and electrodes. Due to the low saturation concentration of oxygen in the acid or alkaline media, the performance of laminar flow-based membraneless fuel cells was primarily limited by mass-transfer of oxygen at the cathode side. This situation could be improved by using air-breathing cathode [20, 21] or high concentration oxidants, such as potassium permanganate [15]. In order to improve the fuel utilization in membraneless micro-fuel cells, it is desirable to recycle the unused fuel. The use of potassium permanganate as the oxidant makes fuel recycling very difficult.

As mentioned above, cost is a major factor for the commercial success of micro fuel cells. The cost factor will become critical, when widespread commercial use of the new broadband devices is established [22]. This paper reports a simple, fast and cost-effective way to fabricate laminar flow-based membraneless fuel cell by combining the rapid prototyping characteristics of laser micromachining and the simple implementation of the membraneless fuel cell concept. The geometry of microstructures on the PMMA substrate can be controlled precisely by adjusting the power and the scanning speed of the laser beam. The technology allows the fabrication of functioning PMMA-based membraneless fuel cells with a gold layer as the current collector and wet-sprayed catalysts on the gold layer as the anode and cathode. The electrochemical performance of the fuel cell was evaluated with formic acid as fuel and hydrogen peroxide as oxidant. To the best knowledge of the authors, the use of hydrogen peroxide in sulfuric acid as oxidant in a membraneless fuel cell is reported for the first time. The use of hydrogen peroxide as oxidant significantly improves the mass-transfer at the cathode side, thus obviously enhancing the fuel cell performance. Furthermore, the use of hydrogen peroxide in sulfuric acid as the oxidant allows simple fuel recycling and better fuel utilization.

2. Experimental procedure

2.1. Fabrication of membraneless fuel cell based on PMMA

Polymthylmethacrylate (PMMA) was chosen as the substrate for many microreaction platforms, because this material offers excellent properties such as low frictional coefficient, high chemical resistance and good electrical insulation [23]. An infrared CO_2 laser (Universal M-300 Laser Platform, Universal Laser Systems Inc., Arizona, USA) was used to engrave microstructures directly on the PMMA substrate. This technique has been proven to be rapid and effective for fabricating microfluidic devices, especially for lab-scale prototyping and small-scale production. The geometry of these structures can be controlled precisely by adjusting the laser power the scanning speed of the laser beam. The ease of varying machining parameters, and thus of the optimization process leads to a relatively short prototyping cycle.

Figure 1(a) shows the different layers of our membraneless fuel cell. This lamination technique was successfully used for making a variety of microfluidic components such as membrane-based micro fuel cells [8], micromixers [14], microvalves [6] and micropumps [7, 23]. The fuel cell is constructed based on three PMMA layers. The top PMMA layer contains two inlets and one outlet. This top layer serves as the electrode support structure as well as the fluidic access for the fuel and the oxidant. The bottom layer works as the electrode support and liquid sealing plate. A 100 nm gold layers were sputtered on the surface of the PMMA sheet (SC7640 sputter coater, Quorum Technologies Ltd) to reduce the contact resistance. This gold layer acts as the current collector on which catalyst inks were wet-sprayed to form the electrode. Before the sputtering process, the surfaces of the PMMA sheets were mechanically treated with fine sandpaper (1200 grit) to improve its surface roughness, and consequently to enhance the adhesion of the gold layer to the substarte. The intermediate layer is a 1-mm thick PMMA sheet for the channel structure. A separation wall was designed in the middle PMMA piece (Fig. 1(a)) to keep the fuel and oxidant apart at the entrance. Both drilling and shaping of the separation wall can be easily realized by CO_2 laser micromachining by adjusting the speed and power of the laser beam. The resulting reaction channel Fig. (1(b)) has a width, depth and length of 1 mm, 1 mm and 5 cm, respectively.

Two different catalyst inks were prepared for the anode and the cathode. In brief, the platinum/ruthenium (Pt/Ru) catalyst (supported on carbon black with metal content of 60% and Pt:Ru = 1:1, from E-Tek) was mixed with Nafion solution (5 wt.% Nafion 5112, from DuPont) in isopropanol with final catalyst concentration of 5 mg/mL and catalyst/Nafion ratio of 7:3. A homogeneous suspension was obtained by ultrasonically mixing the ink at room temperature for 25 minutes. The same procedure was applied to prepare the Pt catalyst ink. The inks were wet-sprayed onto the surface of the Au-coated PMMA substrate using a spray gun (Model 20106, Rich, Japan). Subsequently, the wet-sprayed electrode was heat-treated at 80 °C for 1 hour in an atmospheric air oven to form a smooth electrode film. The final catalyst loading on the electrodes is 4.5 mg/cm^2.

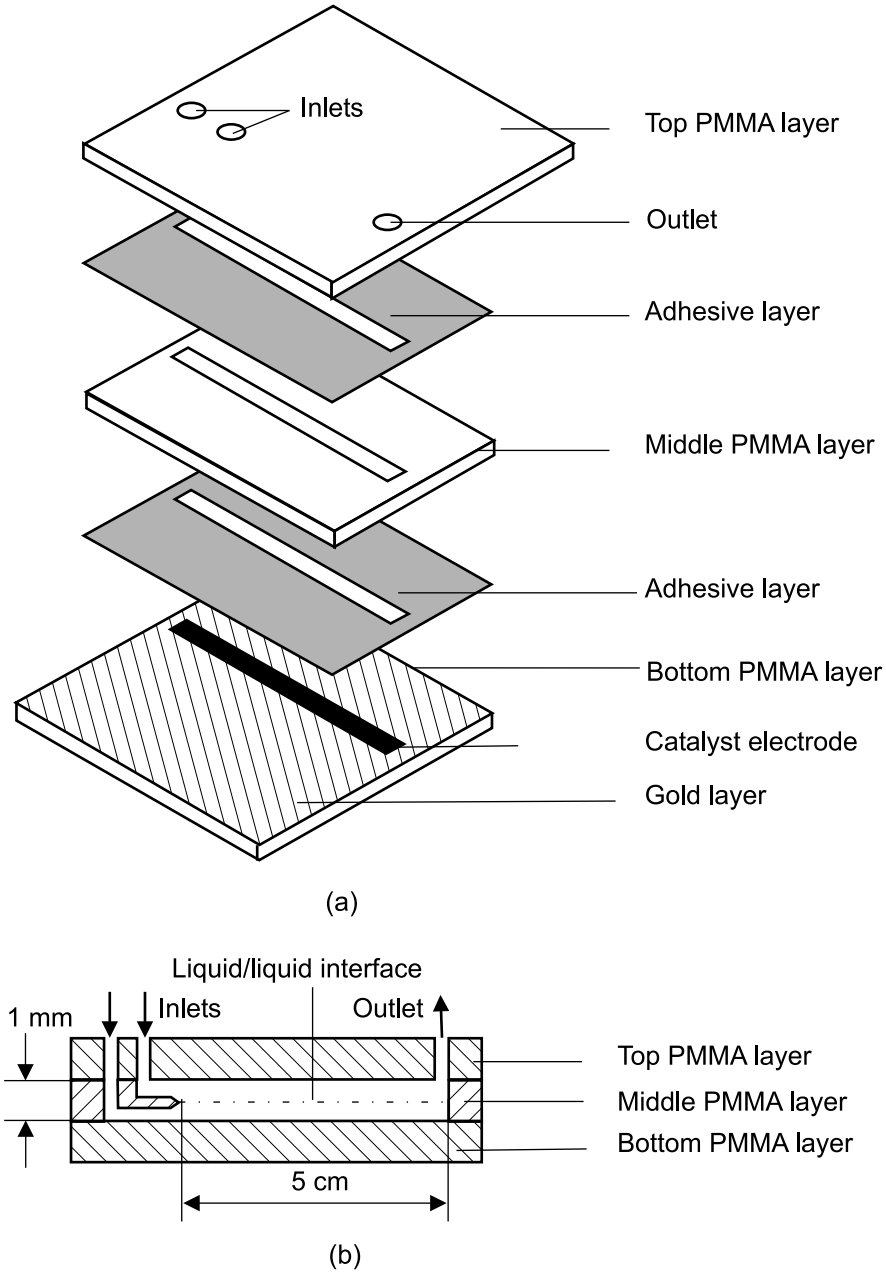

Figure 1. Schematic diagram of the membraneless fuel cell: (a) the different layers, (b) the reaction channel .

The three PMMA layers were bonded together using an adhesive gasket (Adhesives Research, Inc., Arclad 8102 transfer adhesive), which can also be easily cut by the CO_2 laser system. Alignment holes were drilled in all three PMMA layers and the adhesive to allow a fast and accurate assembly of the membraneless micro fuel cell. The fabrication steps are shown in Fig. 2. The top and bottom PMMA plates have gold coating protruded so that the electrical contract to the electrode can be achieved. Polyethylene tubing was glued by epoxy to the inlets and outlet.

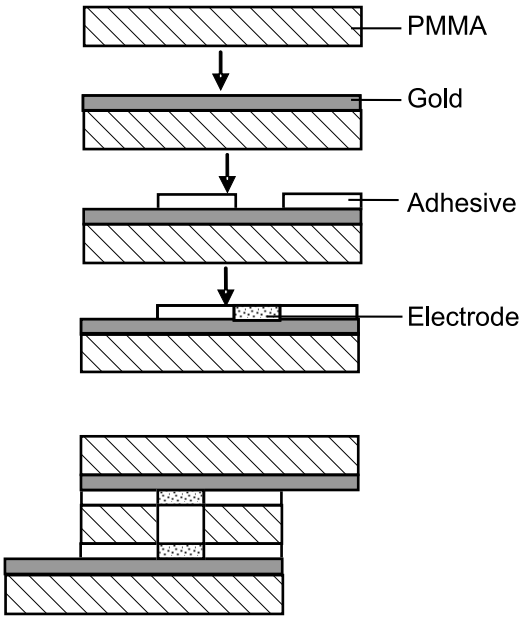

Figure 2. Fabrication steps for the PMMA-based membraneless fuel cell.

2.2. Electrochemical performance evaluation

The power generation process in a membraneless fuel cell follows the electrochemical reactions at anode and cathode. At the anode, formic acid decomposes and creates electrons and protons:

$$\mathrm{HCOOH} \rightarrow \mathrm{CO_2} + 2\mathrm{H^+} + 2\mathrm{e^-} \quad E_0 = 0.22 \text{ V} \tag{1}$$

In the case of saturated oxygen in a H_2SO_4 solution, oxygen reacts with electrons from the cathode and protons from the liquid/liquid interface to form water:

$$\mathrm{O_2} + 4\mathrm{H^+} + 4\mathrm{e^-} \rightarrow 2\mathrm{H_2O} \quad E_0 = 1.229 \text{ V}. \tag{2}$$

In the case of H_2O_2 in a H_2SO_4 solution, the reactions at the cathode are:

$$\begin{aligned} &\mathrm{O_2} + 2H^+ + 2e^- \rightarrow \mathrm{H_2O_2} \qquad E_0 = 0.6 \text{ V} \\ &\mathrm{H_2O_2} + 2\mathrm{H^+} + 2\mathrm{e^-} \rightarrow 2\mathrm{H_2O} \quad E_0 = 1.7 \text{ V}. \end{aligned} \tag{3}$$

Since the diffusion process at the liquid/liquid interface determines the performance of the mebraneless fuel cell, the two key parameters are the Reynolds number:

$$\mathrm{Re} = \frac{UH}{\nu} \tag{4}$$

and the Peclet number:

$$\mathrm{Pe} = \frac{UH}{D_{\mathrm{H^+}}} \tag{5}$$

where U is the mean flow velocity in the reaction channel, H is the channel height, ν is the kinematic viscosity of the fuel/oxidant liquids. For simplification, we assume for an operation temperature of 25 °C a kinematic viscosity of water $\nu = 0.871 \times 10^{-6}$ $\mathrm{m^2 s^{-1}}$ for both fuel and oxidant liquids and a diffusion coefficient of proton

$D_{H^+} = 9.31 \times 10^{-9}$ m^2s^{-1}. With the known volumetric flow rate and channel cross section of 1 mm^2, the Reynolds numbers and the Peclet numbers can be estimated with the above properties.

First, the electrochemical performance of the laminar-flow-based membraneless fuel cell was evaluated. The open circuit potential (OCP) and current-potential curves as a function of volumetric flow rate of the fuel and the oxidant streams were measured by Solartron Electrochemical Analyzer (Model 1287, UK). The flow rates of fuel and oxidant is kept at a fixed ratio of 1:1. The fuel consists of 0.5 M formic acid in 0.1 M H_2SO_4. Two types of oxidant composition are used to study the effect of mass transfer on the fuel cell performance. The first oxidant includes O_2 saturated 0.1 M H_2SO_4. The second oxidant is 0.01 M H_2O_2 in 0.1 M H_2SO_4. A syringe pump (KD Scientific, Model 200) was employed to precisely supply the fuel and oxidant streams into the fuel cell channel. The flow rates in our experiments range from 0.2 to 1.6 ml/min. The fuel cell was operated at the room temperature of 25 °C. Before the testing process, the formic acid solution was degassed with N_2 for 30 minutes and oxygen was bubbled into sulfuric acid for more than two hours to saturate oxygen in the sulfuric acid solution.

3. Results and Discussions

The PMMA based membraneless fuel cell was first tested with 0.5 M HCOOH in 0.1 M H_2SO_4 as fuel and O_2 saturated in 0.01 M H_2SO_4 as oxidant to understand its functionality. Figure 3(a) shows the effect of the volumetric flow rate of the fuel and oxidant streams on the fuel cell polarization. The cell polarization curves were measured over a broad range of volumetric flow rate from 0.4 to 1.6 ml/min. The current densities and power densities were evaluated based on the real geometric area of the electrodes. When the volumetric flow rate was lower than 0.4 ml/min (Re=7.65, Pe=716), the open circuit potential was close to zero so that no power was generated. At this low flow rate, molecular diffusion dominates over convection. Thus, severe fuel crossover phenomenon occurred at the liquid-liquid interface. Our experimental results agree well with the numerical prediction reported by Chen et al. [25]. The upper limit of 1.6 ml/min (Re=30.6, Pe=2860) is determined by the transition to instability. Above this critical point, the flow is not stable due to the dominant convective flow at high Reynolds number. The solubility of oxygen in the water-based electrolyte at room temperature is as low as around 0.5 mM [15]. Thus, obvious limiting current densities were observed from the polarization curves due to the insufficient supply of oxygen from the oxidant stream to the cathode. The limiting current density increased with the increase of the volumetric flow rate. An increment in limiting current density of 0.2 mA/cm^2 was achieved, when volumetric flow rate increased from 0.4 to 0.6 mL/min. The increment was significantly reduced to 0.05 mA/cm^2 when volumetric flow rate increased from 1.4 to 1.6 mL/min.

From the polarization curves, the output power densities of the membraneless fuel cell at various volumetric flow rates are depicted in Fig. 3(b). The higher the volumetric

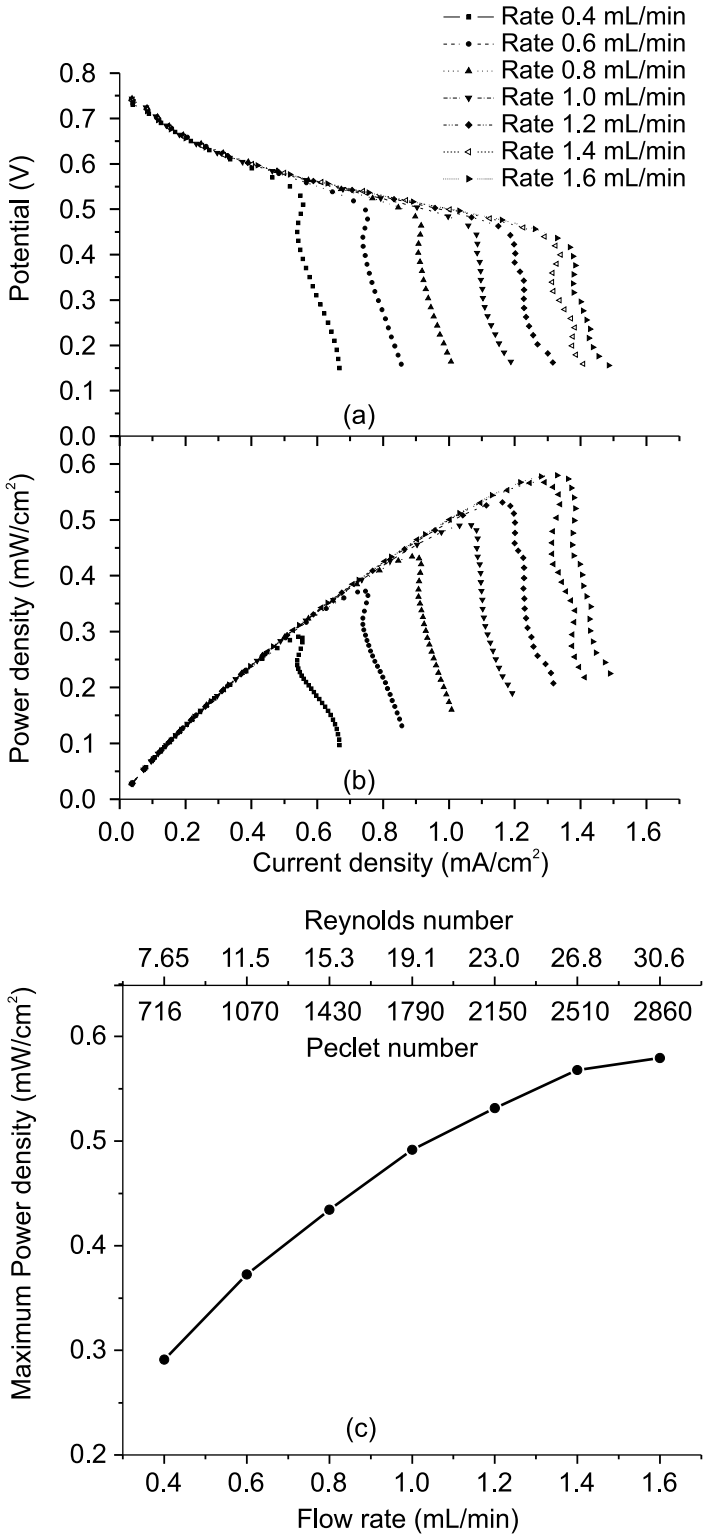

Figure 3. The performance of the PMMA-based membraneless fuel cell with different flow rate: (a) I-V curves; (b) power density curves; (c) the maximum power density versus the flow rate. The Fuel stream is 0.5 M formic acid in 0.1 M H_2SO_4 and the oxidant stream is 0.01 M H_2SO_4 saturated with oxygen.

flow rate, the faster the cathode depletion zone is filled with fresh oxygen contained liquid so that higher current can be drawn from the fuel cell. As a result, in the volumetric flow rate range of 0.4-0.6 ml/min or the Reynolds number range of 7.65-30.6, the maximum power densities are obviously improved with increasing the flow rate. Once the supply of the oxygen into cathode electrode cannot maintain the reaction, a limiting current would be observed. Thus, as shown in Fig. 3(c), the maximum power density increment of 81.2 μW/cm^2 with an increase of flow rate from 0.4ml/min to 0.6 ml/min reduces to 11.5 μW/cm^2 with an increase of flow rate from 1.4 ml/min to 1.6 ml/min. The periodic fluctuation observed on the polarization curves at high volumetric flow rate of 1.4 ml/min and 1.6 ml/min could be cause by the stepping motion of the syringe pump.

Under the current cell geometry and operating conditions, there are two challenges in the development of a high-performance membraneless fuel cell. The first challenge is the low performance of the fuel cell due to the mass transport limitation of saturated oxygen on the cathode side. The second challenge is the very low fuel utilization. For the first time, hydrogen peroxide in sulfuric acid was used as the oxidant in the membraneless fuel cell. The use of the hydrogen peroxide provides much higher oxidant content than oxygen saturated sulfuric acid and makes it possible to recycle the fuel. Figure 5 illustrates the performance of the fuel cell with different volumetric flow rate using 0.01 M H_2O_2 in 0.01 M H_2SO_4 as the oxidant. The fuel cell can operate stably in the volumetric flow rate range of 0.4 ml/min to 1.6 ml/min. Similar to the results presented in Fig. 3(a), the current density is enhanced gradually with the increase of the volumetric flow rate as shown in Fig. 4(a). Compared with oxygen saturated sulfuric acid, it is obvious that the fuel cell with hydrogen peroxide as oxidant could deliver a much higher power density. When the flow rate was 1.6 mL/min, the maximum power density was as high as 1.92 mW/cm^2, which is comparable with the Y-shaped membraneless fuel cell using 0.144 M potassium permanganate as oxidant and 2.1 M formic acid as fuel [15]. However, as can be seen in polarization curves shown in Fig. 4(a), the fluctuation at low current density becomes obvious at high volumetric flow rates. This phenomenon could be caused by the generation of oxygen bubbles during the decomposing process of H_2O_2 at the cathode surface, which disturb the laminar streams under the high flow rate condition. Output power densities of the membraneless fuel cell with H_2O_2-based oxidant are summarized in Fig. 4(b) and Fig. 4(c).

Figure 5(a) shows the stability of the open circuit potential (OCP) in HCOOH/O_2 and HCOOH/H_2O_2 membraneless fuel cell systems. The data was evaluated at a total volumetric flow rate of 1.0 mL/min of both fuel and oxidant streams. While the OCP of the HCOOH/O_2 system is very stable during the testing experiments, the OCP of HCOOH/H_2O_2 system fluctuates. This phenomenon may be caused by the chemical decomposition of H_2O_2 to gaseous O_2 on the cathode catalyst surface. The oxygen bubbles disturb the laminar flow and subsequently leads to the fluctuation of OCP. Furthermore, it is apparent that the OCPs of both HCOOH/O_2 and HCOOH/H_2O_2 system is much lower than their thermodynamic values. That means, the reaction kinetics of HCOOH on the anode catalyst surface is a slow process. Under the open

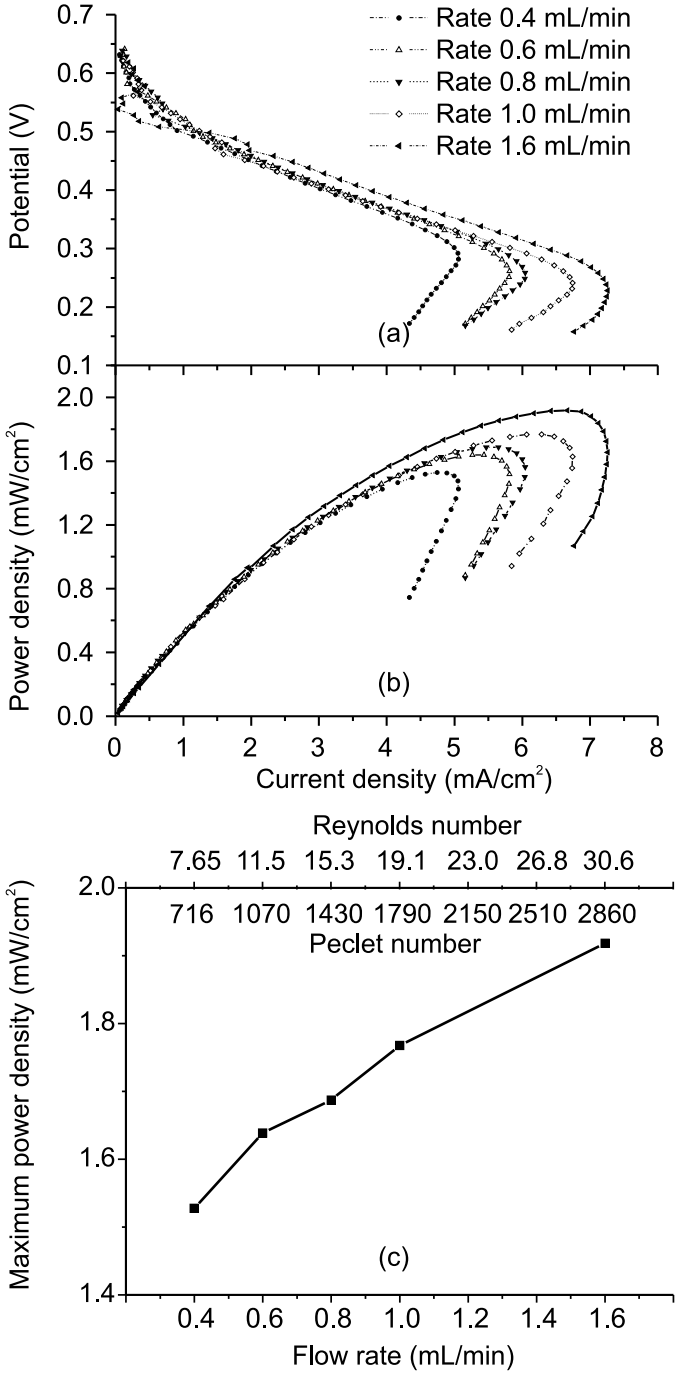

Figure 4. The performance of the PMMA-based membraneless fuel cell with different flow rate: (a) I-V curves and; (b) power density curves; (c) the maximum power density versus the flow rate. 0.5 M formic acid in 0.01 M H_2SO_4 is fuel and 0.01 M H_2O_2 in 0.01 M H_2SO_4 is oxidant.

circuit condition, the equilibrium state of the HCOOH reaction is not established on the catalyst surface. Fig. 5(b) shows the mean OCP values of HCOOH/O_2-based and HCOOH/H_2O_2-based membraneless fuel cell systems as a function of volumetric flow rates. The OCP values are almost independent of the volumetric flow rate. The

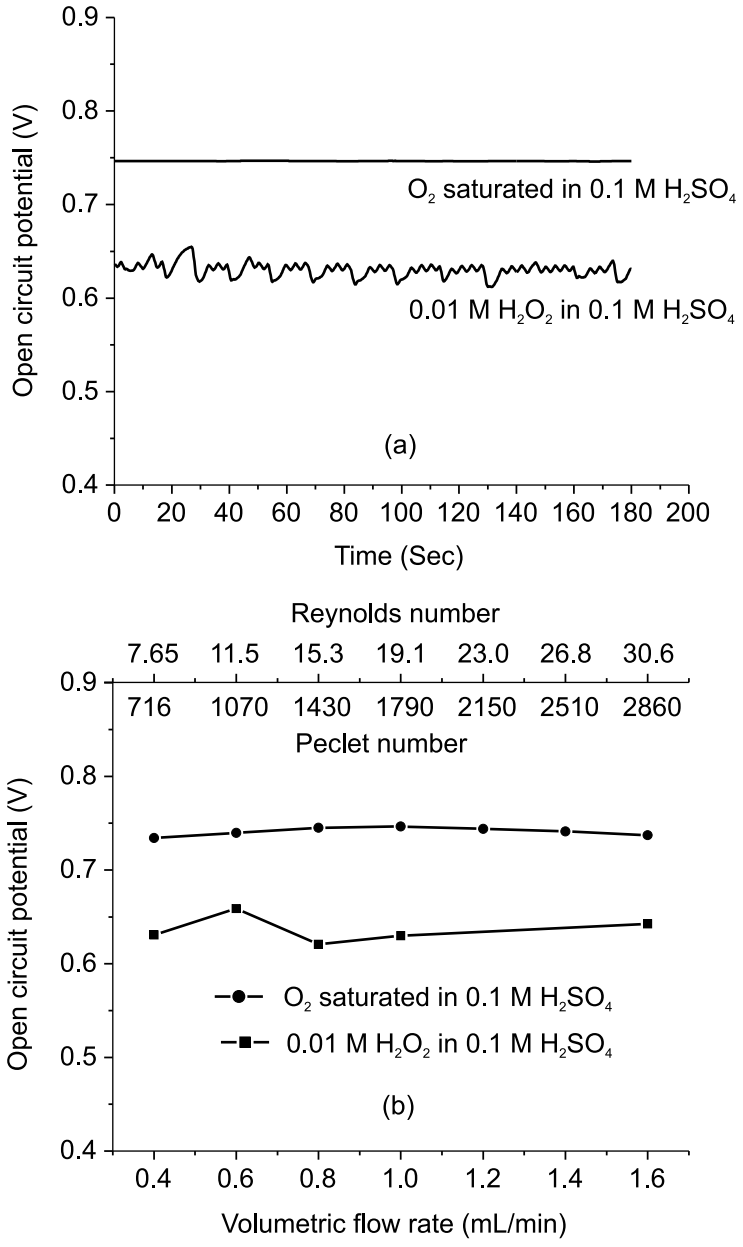

Figure 5. (a) The open circuit potential with volumetric flow rate 1.0 ml/min; (b) Open circuit potential as a function of volumetric flow rate.

fluctuation of the OCP values at various volumetric flow rates is more obvious in the $HCOOH/H_2O_2$ system than that in $HCOOH/O_2$ system. This phenomenon can be explained by the disturbance of oxygen bubbles on the cathode's catalyst surface. Figure 6 shows the stability of the PMMA based membraneless fuel cell under polarization condition. With the exception of some fluctuations of the output current, the fuel cell can operate stably in both $HCOOH/O_2$ and $HCOOH/H_2O_2$ systems during the testing period.

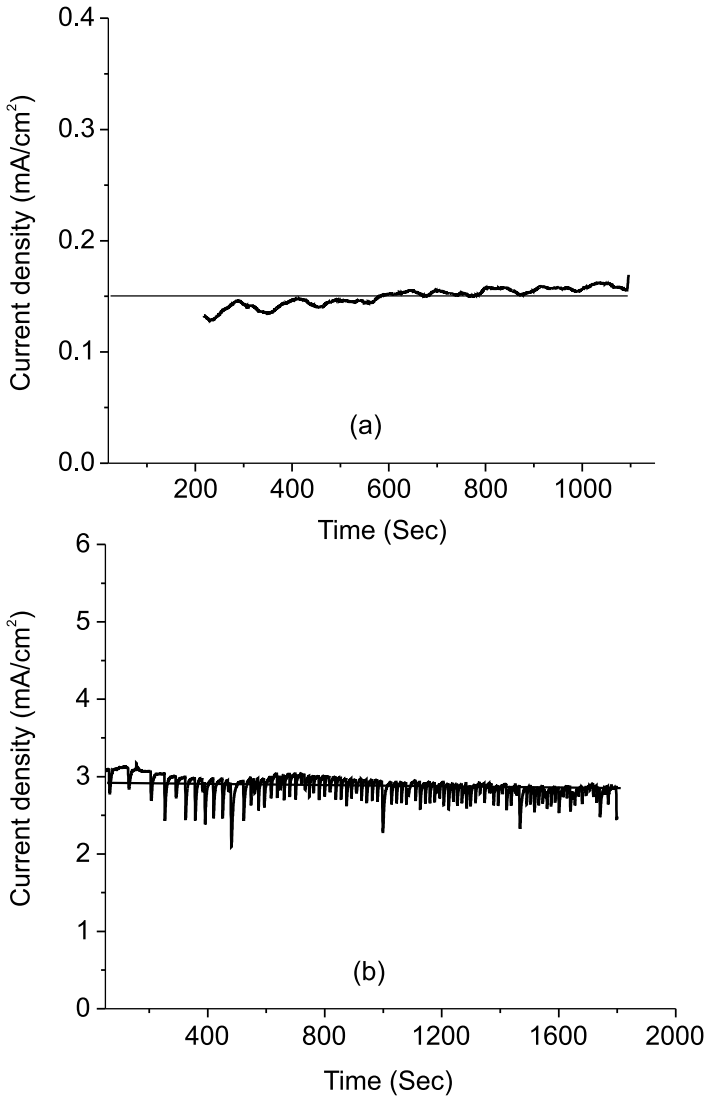

Figure 6. Stability of the membraneless fuel cell operating at voltage of 0.4 V with flow rate 1.0 mL/min using (a) O_2 saturated in sulfuric acid as oxidant; (b) H_2O_2 in sulfuric acid as oxidant.

4. Conclusions

In this paper, we designed, fabricated and tested a novel membraneless fuel cell based on polymeric micromachining. A fully PMMA-based membraneless fuel cell was fabricated using CO_2 laser micromachining. The fuel cell electrodes were fabricated by wet-spraying the catalyst inks onto the top and bottom gold-coated PMMA substrates. The middle PMMA layer forms the reaction microchannel. The two laminar streams containing fuel and oxidant are kept separated in this microchannel but remain in diffusional contact. The electrochemical performance of the membraneless fuel cell was characterized using formic acid (HCOOH) as fuel and saturated O_2 as well as H_2O_2 as oxidant. The results demonstrated that the developed membraneless fuel cell can stably operate in a wide range of volumetric flow rates of fuel and oxidant. In the

Reynolds number range of 7.65 to 30.6, the higher the volumetric flow rate, the higher is the maximum power density. Beyond this range, the fuel cell cannot operate stably due to fuel cross-over at low flow rates (Re¡7.65) and instability at high flow rates (Re¿30.6) of the fuel and oxidant streams. Optimal operation flow rate should be a trade-off between dominant convection and stable flow. The poor solubility of O_2 in the water- based electrolyte at room temperature limits the power output. H_2O_2 dissolved in H_2SO_4 was employed to improve the mass-transfer of the oxidant on the cathode side, thus significantly enhancing the electrochemical performance of the membraneless fuel cell. The maximum power density can reach 1.98 mW/cm^2 in 0.5 M HCOOH+0.1 M H_2SO_4/0.01 M H_2O_2+0.1 M H_2SO_4 system, which is more than three times of 0.58 mW/cm^2 in 0.5 M HCOOH+0.1 M H_2SO_4/saturated O_2+0.1 M H_2SO_4 system at volumetric flow rate of 1.6 mL/min.

References

[1] Nguyen N T and Chan S H 2006 Micromachined polymer electrolyte membrane and direct methanol fuel cells - a review *J. Micromech. Microeng.* **16** R1-R12

[2] Yu J *et al* 2003 Fabrication of miniature silicon wafer fuel cells with improved performance *J. Power Sources* **124** 40-6

[3] Lee S J et al 2002 Design and fabrication of a micro fuel cell array with "flip-flop" interconnection *J. Power Sources* **112** 410-418

[4] Motokawa S *et al* 2004 MEMS-based design and fabrication of a new concept micro direct methanol fuel cell (μ-DMFC) *Electrochemistry Communications* **6** 562-565

[5] Yeom J *et al* 2006 Passive direct formic acid microfabricated fuel cells *J. Power Sources* **160** 1058-64

[6] Nguyen N T *et al* 2004 Micro check valves for integration into polymeric microfluidic devices *J. Micromech. Microeng.* **14** 69-75

[7] Truong T Q and Nguyen N T 2004 A polymeric piezoelectric micropump based on lamination technology *J. Micromech. Microeng.* **14** 632-638

[8] Chan S H *et al* 2005 Development of a polymeric micro fuel cell containing laser-micromachined flow channels *J. Micromech. Microeng.* **15** 231-6

[9] Scott K *et al* 1999 The impact of mass transport and methanol crossover on the direct methanol fuel cell *J. Power Sources* **83** 204-16

[10] Ren X M *et al* 2000 Recent advances in direct methanol fuel cells at Los Alamos National Laboratory *J. Power Sources* **86** 111-116

[11] Mano N, Mao F, Heller A 2003 Characteristics of a miniature compartment-less glucose-O2 biofuel cell and its operation in a living plant *J. Am. Chem. Soc.* **125** 6588-94

[12] Mano N, Mao F, Heller A 2002 A miniature biofuel cell operating in a physiological buffer *J. Am. Chem. Soc.* **124** 12962-63

[13] Ferrigno R *et al* 2002 Membraneless vanadium redox fuel cell using laminar flow *J. Am. Chem. Soc.* **124** 12930-31

[14] Wu Z G abd Nguyen NT 2004 Convective-diffusive transport in parallel lamination micromixers *Microfluidics and Nanofluidics* **1** 208-17

[15] Choban E R *et al* 2004 Microfluidic fuel cell based on laminar flow *J. Power Sources* **128** 54-60

[16] Choban E R *et al* 2005 Membraneless laminar flow-based micro fuel cells operating in alkaline, acidic, and acidic/alkaline media *Electrochimica Acta* **50** 5390-8

[17] Choban E R *et al* 2005 Characterization of limiting factor in laminar flow-Based membraneless microfuel cells *Electrochemical and Solid-State Letters* **8** A348-52

[18] Cohen J L *et al* 2005 Fabrication and preliminary testing of a planar membraneless microchannel fuel cell *J. Power Sources* **139** 96-105
[19] Cohen J L *et al* 2005 A dual electrolyte H_2/O_2 planar membraneless microchannel fuel cell system with open circuit potentials in excess of 1.4V *Langmuir* **21** 3544-50
[20] Jayashree R S *et al* 2005 Air-breathing Laminar flow-based microfluidic fuel cell *J. Am. Chem. Soc.* **127** 16758-9
[21] Jayashree R S *et al* 2006 Air-breathing laminar flow-based direct methanol fuel cell with alkaline electrolyte *Electrochemical and Solid-State Letters* **9** A252-56
[22] Dyer C K 2002 Fuel cells for portable application *J. Power Sources* **106** 31-4
[23] Nguyen N T and Truong T Q 2004 A fully polymeric micropump with piezoelectric actuator it Sensors and Actuators B: Chemical **1** 137-43
[24] Yang W 2006 Nanostructured silver catalyzed nickel foam cathode for an aluminum- hydrogen peroxide fuel cell *J. Power Sources* **160** 1420-4
[25] Chen F *et al* 2007 Analysis of membraneless formic acid microfuel cell using a planar microchannel *Electrochimica Acta* **52** 2506-14